

1 **Synthesis of defined oligohyaluronates-decorated liposomes and interaction with lung**  
2 **cancer cells**

3 Maria Emilia Cano <sup>a</sup>, David Lesur <sup>a</sup>, Valeria Bincoletto <sup>b</sup>, Elena Gazzano <sup>c</sup>, Barbara Stella <sup>b</sup>,  
4 Chiara Riganti <sup>c</sup>, Silvia Arpicco <sup>b,\*</sup>, José Kovensky <sup>a,\*</sup>

5 <sup>a</sup> *Laboratoire de Glycochimie, des Antimicrobiens et des Agroressources CNRS UMR 7378,*  
6 *Université de Picardie Jules Verne, 33 rue Saint Leu, 80039 Amiens, France*

7 <sup>b</sup> *Department of Drug Science and Technology, University of Torino, Via Giuria 9, 10125 Torino,*  
8 *Italy*

9 <sup>c</sup> *Department of Oncology, University of Torino, Via Santena 5/bis, 10126 Torino, Italy*

10 \*Corresponding authors: [silvia.arpicco@unito.it](mailto:silvia.arpicco@unito.it); [jose.kovensky@u-picardie.fr](mailto:jose.kovensky@u-picardie.fr)

11

12 In this work hyaluronic acid (HA) oligosaccharides with degree of polymerization (DP) 4, 6  
13 and 8, obtained by enzymatic depolymerization of HA, were conjugated to a PEG-  
14 phospholipid moiety. The products (HA-DP4, HA-DP6 and HA-DP8) were used to prepare  
15 decorated liposomes. The cellular uptake of HA-DP4, HA-DP6 and HA-DP8-decorated  
16 fluorescently labelled liposomes was significantly higher (12 to 14-fold) in lung cancer cell  
17 lines with high CD44 expression than in those with low CD44 expression, suggesting a  
18 receptor-mediated entry of HA-conjugated formulations. Competition assays showed that  
19 the uptake followed this rank order: HA-DP8>HA-DP6>HA-DP4 liposomes. Moreover, they  
20 are capable of a faster interaction with CD44, followed by phagocytosis, than HA  
21 liposomes obtained from HA of higher molecular weight (4800 and 14800 Da). HA-DP4,  
22 HA-DP6 and HA-DP8-liposomes did not show cytotoxicity or inflammatory effects. Overall,  
23 we propose our new HA-DP oligosaccharides as biocompatible and effective tools for a  
24 potential drug delivery to CD44-positive cells.

25 **Keywords:** Hyaluronic acid; oligosaccharides; liposomes; HA-CD44 interaction

26 **1. Introduction**

27 Hyaluronic acid (HA) is a widely distributed extracellular matrix polysaccharide of the  
28 glycosaminoglycan family. It is a polymer of high molecular weight composed of  
29 alternating glucuronic acid (GlcA) and *N*-acetylglucosamine (GlcNAc) units forming a  
30 repeating sequence of the disaccharide  $\beta$ -D-GlcA-(1 $\rightarrow$ 3)- $\beta$ -D-GlcNAc-(1 $\rightarrow$ 4). This  
31 biomolecule is involved in the regulation of inflammation, tumor development and healing  
32 processes through its interaction with different proteins (Fuster & Esko, 2005; Toole,  
33 2004).

34 HA is considered as a key biomarker of specific cancers, because CD44, the main receptor  
35 of HA at the cell surface, is overexpressed on different solid (colon, ovarian, breast, lung)  
36 tumors and leukemias. The binding of HA to CD44 modulates the regulation and the  
37 proliferation of cancer cells. Recently, it has been reported that the repeating sequence of  
38 HA provides multiple binding sites for CD44 binding, inducing CD44 clustering, an event  
39 related to tumor progression and inflammation processes (Yang et al., 2012).

40 This binding has prompted researchers to use HA-phospholipid conjugates to construct  
41 liposomes able to target tumor cells through the CD44 receptor. In previous works, it has  
42 been shown that such liposomes can successfully bind to cells, and if they are loaded with  
43 anticancer drugs as gemcitabine or doxorubicin derivatives, they can be internalized and  
44 delivered efficiently. (Arpicco et al., 2013; Dalla Pozza et al., 2013; Gazzano et al., 2019;  
45 Marengo et al., 2019).

46 Like other polymers, macromolecular HA is not homogeneous: indeed, it is composed of  
47 multiple chains of different length, with an average molecular weight of about  $10^6$  Da.  
48 Oligosaccharides of lower molecular weight that can be obtained by chemical or  
49 enzymatic depolymerization, also bind CD44. However, it has been reported that a  
50 mixture of oligosaccharides with a degree of polymerization (DP) 4-20 exhibits pro-  
51 inflammatory effects, while HA polysaccharide exerts opposite effects (Gao, Yang, Mo,  
52 Liu, & He, 2008). This difference has been interpreted in terms of monovalent vs.

53 multivalent interactions. Clustering of CD44 would require multivalent HA-CD44 binding  
54 occurring with the HA polymer, whereas HA oligosaccharides could only allow monovalent  
55 interactions, thus preventing the receptor clustering. (Yang et al., 2012)

56 In this paper, we explore the use of small HA oligosaccharides of defined structure and  
57 purity. Our approach involved the chemical modification of these oligosaccharides (DP4, 6  
58 and 8) and conjugation to a phospholipid moiety. These conjugates were used to prepare  
59 liposomes, which present at the surface a multivalent arrangement of these small  
60 oligosaccharides. After complete characterization of the liposomes, the cellular uptake by  
61 human lung cancer cells, the cell viability and the inflammatory profile were studied.

## 62 **2. Materials and methods**

### 63 *2.1. Materials*

64 Fetal bovine serum (FBS), fluorescein-5-(and-6)-sulfonic acid trisodium salts and culture  
65 medium were from Invitrogen Life Technologies (Carlsbad, CA). Plasticware for cell  
66 cultures was from Falcon (Becton Dickinson, Franklin Lakes, NJ). All the phospholipids  
67 were provided by Avanti Polar-Lipids distributed by Sigma-Chemical Co (St. Louis, MO).  
68 The protein content in cell extracts was assessed with the BCA kit from Sigma Chemical  
69 Co. Unless otherwise specified, all the other reagents were purchased from Sigma  
70 Chemical Co.

### 71 *2.2. Analytical methods*

72  $^1\text{H}$  NMR (400 MHz) and  $^{13}\text{C}$  NMR (101 MHz) spectra were recorded in  $\text{D}_2\text{O}$ . The proton and  
73 carbon signal assignments were determined from decoupling experiments. Thin layer  
74 chromatography (TLC) was performed on Silica F254 and detection by UV light at 254 nm  
75 or by charring with sulfuric acid in ethanol. High-resolution electrospray mass spectra in  
76 the positive ion mode were obtained on a Q-TOF Ultima Global hybrid quadrupole/time-  
77 of-flight instrument, equipped with a pneumatically assisted electrospray (Z-spray) ion  
78 source and an additional sprayer (Lock Spray) for the reference compound. The source

79 and desolvation temperatures were kept at 80 and 150 °C, respectively. Nitrogen was  
80 used as the drying and nebulizing gas at flow rates of 350 and 50 L/h, respectively. The  
81 capillary voltage was 3.5 kV, the cone voltage 100 V and the RF lens<sup>1</sup> energy was  
82 optimized for each sample (40 V). Lock mass correction, using appropriate cluster ions of  
83 sodium iodide (NaI)<sub>n</sub>Na<sup>+</sup>, was applied for accurate mass measurements. The mass range  
84 was typically 50-2050 Da and spectra were recorded at 2 s/scan in the profile mode at a  
85 resolution of 10000 (FWMH).

### 86 *2.3. Enzymatic hydrolysis of hyaluronic acid*

87 Sodium hyaluronate (2 g) was dissolved in 0.1 M sodium acetate buffer (41 mL, pH 4.5) at  
88 37 °C and bovine testes hyaluronidase (BTH, 12800 U) was added. After stirring for 2 days  
89 at 37 °C, 6000 U of enzyme were added. The addition of enzyme was repeated until TLC  
90 (n-butanol/formic acid/water, 2:2:1) showed no further changes (15 days). The solution  
91 was heated at 80°C for 5 min, filtered to remove the denatured enzyme, and freeze-dried.  
92 The crude product was desalted on Sephadex LH-20 using water as eluent. Analytical  
93 anion exchange chromatography (HPAEC) of the oligosaccharide mixture showed the  
94 presence of DP<sub>4</sub>, 6 and 8 as the main products.

### 95 *2.4. Purification of oligosaccharides of DP<sub>4</sub>, DP<sub>6</sub> and DP<sub>8</sub> of hyaluronic acid*

96 The separation of the oligosaccharides was performed on a HPLC Waters autopurification  
97 system (Waters, France) equipped with a 1525 binary pump coupled to a 2998 PDA  
98 detector (Waters, France), and a SEDEX LT-ELSD LC detector (Sedere, France). The run was  
99 performed at room temperature, the compounds were loaded on a TSKgel DEAE 5PW  
100 column (10 µm particle size, 200 mm x 50 mm) and the sample injection volume was 700  
101 µl (aqueous solutions of compounds at 140 mg/mL). The mobile phase consisted of 1mM  
102 ammonium formate (solvent A) and 1M ammonium formate (solvent B). The composition  
103 of the mobile phase varied during the run as follows:

104 *Condition prep:* A:B: 0-20 min (100:0 to 85:15 v/v), 20-50 min (85:15 to 62:38 v/v), 50.01-  
105 60 min (0:100 v/v) at a flow rate of 30 mL/min.

106 Data acquisition and processing were performed with MassLynx V4.1 software.

107 After lyophilization, compounds **1a**, **1b** and **1c** were obtained in pure form in 14%, 16%  
108 and 17% yield, respectively.

### 109 *2.5. Direct azidation of the oligohyaluronans of DP4, 6 and 8*

110 Compounds **2a-c** were synthesized using a previously described methodology (Köhling et  
111 al., 2019). Briefly, 2-chloro-1,3-dimethylimidazolium (DMC, 118 mg, 0.7 mmol) was  
112 added to a solution of oligohyaluronans (0.07 mmol), *N*-methylmorpholine (212 mg, 2.1  
113 mmol) and NaN<sub>3</sub> (273 mg, 4.2 mmol) in water at 0 °C. The mixture was stirred at room  
114 temperature for 30 h and then was evaporated under reduce pressure. The 1-  
115 azidooligosaccharides **2a** and **2b** were purified on a Sephadex LH-20 column using  
116 deionized water to give the pure tetra- and hexasaccharide derivatives in 68% and 65%  
117 yield, respectively. The analytical data were in accordance to those previously reported  
118 (Köhling et al., 2019, 2016). The octasaccharide derivative was desalted using a Cellulose  
119 Ester (CE) dialysis membrane (MWCO: 100-500 Da) to afford **2c** (69 mg, 63% yield). <sup>1</sup>H  
120 NMR (D<sub>2</sub>O, 400 MHz) δ 4.80 (1H), 4.50-4.47 (m, 3H), 4.44-4.40 (m, 4H), 3.94-3.71 (m, 24H),  
121 3.63-3.51 (m, 12H), 3.40-3.32 (m, 4H), 2.04 (s, 3H, Ac), 2.03 (2s, 9H, Ac); <sup>13</sup>C NMR (D<sub>2</sub>O,  
122 101 MHz) δ 174.9 (CO), 103.0, 102.9, 100.7 (C-1), 88.5 (C-1 N<sub>3</sub>), 82.9, 82.4, 81.9, 79.9, 77.4,  
123 75.7, 75.5, 75.4, 75.3, 75.2, 73.6, 72.6, 72.3, 71.5, 68.4, 68.3, 60.5, 54.3, 54.2, 22.4; ESI-  
124 HRMS (positive ion): *m/z* [M+Na]<sup>+</sup> calcd for (C<sub>56</sub>H<sub>85</sub>N<sub>7</sub>O<sub>44</sub>Na<sup>+</sup>): 1582.4527; found:  
125 1582.4531.

### 126 *2.6. General procedure for click reaction*

127 DSPE-PEG(2000)-DBCO **3** (10 μmol) was dissolved in water (473 μL). An aqueous solution  
128 of the sugar residues (10 μmol in 190 μL of water) was added, the mixture was stirred at  
129 room temperature for 1 h and then was lyophilized. Compound **4a**: ESI-HRMS (neg.): *m/z*

130  $[M-2H]^{3-}$  calcd. for (C<sub>179</sub>H<sub>316</sub>N<sub>8</sub>O<sub>78</sub>P<sup>3-</sup>): 1285.6888; found: 1285.6915. Compound **4b**: ESI-  
131 HRMS (neg.):  $m/z$   $[M-H]^{2-}$  calcd. for (C<sub>193</sub>H<sub>338</sub>N<sub>9</sub>O<sub>89</sub>P<sup>2-</sup>): 2118.5969; found: 2118.6045.  
132 Compound **4c**: ESI-HRMS (neg.):  $m/z$   $[M-2H]^{3-}$  calcd. for (C<sub>207</sub>H<sub>358</sub>N<sub>10</sub>O<sub>100</sub>P<sup>3-</sup>): 1538.4325;  
133 found: 1538.4259.

## 134 2.7. Liposomes preparation and characterization

135 Liposomes were prepared by the thin lipid film hydration and extrusion method.  
136 Chloroform solution of 1,2-distearoyl-*sn*-glycero-3-phosphocholine (DSPC), cholesterol  
137 (CHOL) and 1,2-distearoyl-*sn*-glycero-phosphoethanolamine-N-[amino(polyethylene  
138 glycol)-2000] (mPEG2000-DSPE) in a molar ratio 75:20:2 was mixed and evaporated under  
139 reduce pressure to obtain a thin lipid film. The resulting lipid film was hydrated with a 20  
140 mM 4-(2-hydroxyethyl)piperazine-1-ethanesulfonic acid (HEPES) buffer (pH 7.4) and  
141 vortexed for 10 min to obtain a suspension of multilamellar liposomes. The resulting  
142 suspension was then extruded (Extruder, Lipex, Vancouver, Canada) 10 times under  
143 nitrogen through 200 nm polycarbonate filter at 60°C.

144 To prepare decorated liposomes (LipoHA-DP4, LipoHA-DP6, LipoHA-DP8), the same  
145 method was used. Lipid films were made up of DSPC/CHOL/mPEG2000-DSPE (75:20:2  
146 molar ratio) and then hydrated using solution of the different HA-DP conjugates **4a**, **4b**  
147 and **4c** (3 molar ratio) in HEPES buffer.

148 Fluorescently labeled liposomes were prepared as described above by adding 10 mM  
149 solution of fluorescein-5-(and-6)-sulfonic acid trisodium salts in HEPES buffer during the  
150 hydration of the lipid film. The untrapped fluorescein was removed by gel filtration  
151 using Sepharose® CL-4B column eluting with HEPES buffer. Liposomes were stored at 4 °C.

152 The mean particle size and polydispersity index (PI) of the liposomes were determined at  
153 25 °C by quasi-elastic light scattering (QELS) using a nanosizer (Nanosizer Nano Z, Malvern  
154 Inst., Malvern, UK). The selected angle was 173° and the measurement was made after

155 dilution of the liposomes suspension in MilliQ® water. Each measure was performed in  
156 triplicate.

157 The particle surface charge of liposomes was investigated by zeta potential measurements  
158 at 25 °C applying the Smoluchowski equation and using the Nanosizer Nano Z.  
159 Measurements were carried out in triplicate.

## 160 *2.8. Cell cultures*

161 Human epithelial lung cells BEAS-2B, human non-small cell lung cancer cells A549, NCI-  
162 H1385, NCI-H1975, NCI-H1650, NCI-H228, Calu-3 were purchased from ATCC (Manassas,  
163 VA). Cells were grown in RPMI-1640 medium, supplemented with 10% v/v FBS and 1%  
164 penicillin-streptomycin, at 37 °C, 5% CO<sub>2</sub>, in a humidified atmosphere.

## 165 *2.9. Flow cytometry*

166  $1 \times 10^6$  cells were rinsed and fixed with 2% w/v paraformaldehyde (PFA) for 2 min, washed  
167 three times with PBS and stained with the anti-CD44 antibody (Abcam, Cambridge, UK) for  
168 1 h on ice, followed by an AlexaFluor 488-conjugated secondary antibody (Millipore,  
169 Burlington, MA) for 30 min.  $1 \times 10^5$  cells were analyzed with EasyCyte Guava™ flow  
170 cytometer (Millipore), equipped with the InCyte software (Millipore). Control experiments  
171 included incubation with non-immune isotype antibody.

## 172 *2.10. Cellular uptake*

173  $1 \times 10^5$  cells were seeded into a 96-well black plate, let to adhere for 6 h and incubated at  
174 different time points with the fluorescently labeled liposomes as indicated in the Results  
175 section. Cells were washed twice with PBS and rinsed with 300 µl PBS. The intracellular  
176 fluorescence, an index of liposome uptake, was measured using a Synergy HT Microplate  
177 Reader (Bio-Tek Instruments, Winooski, VT), using  $\lambda$  excitation 460 nm and  $\lambda$  emission 530  
178 nm. Cells were then detached with trypsin/EDTA, sonicated and used for the measure of

179 intracellular protein contents. Results were expressed as fluorescence units (FU)/mg  
180 cellular proteins.

#### 181 *2.11. Cell viability*

182  $1 \times 10^4$  cells were seeded into a 96-well white plate, let to adhere for 6 h and incubated for  
183 72 h with the liposomes as indicated in the Results section. Cell viability was measured by  
184 the ATPlite Luminescence Assay System (PerkinElmer, Waltham, MA), as per  
185 manufacturer's instructions. Results were analyzed by a Synergy HT Microplate Reader.  
186 The luminescence units of the untreated cells were considered 100%; the luminescence  
187 units of the other experimental conditions were expressed as percentage versus  
188 untreated cells.

#### 189 *2.12. Cytokine measurement*

190 1 ml of cell culture supernatant was collected after 24 h treatment and probed with the  
191 Human Inflammation Antibody Array – Membrane (Abcam), as per manufacturer's  
192 instructions. Results were quantified by densitometry analysis of each dot blot, using  
193 Image J software ([www.imagej.nih.gov](http://www.imagej.nih.gov)). The dot blot density of untreated cells was  
194 considered 1; results of the treatment conditions were expressed as fold change (density  
195 of dot blot for each experimental condition/density of dot blot in untreated cells for the  
196 same cytokine).

#### 197 *2.13. Statistical analysis*

198 All data in the text and figures are provided as means  $\pm$  SD. The results were analyzed by a  
199 one-way analysis of variance (ANOVA) and Tukey's test.  $p < 0.05$  was considered  
200 significant.

### 201 **3. Results and discussion**

#### 202 *3.1. Enzymatic treatment of hyaluronate and purification of hyaluronic oligosaccharides*

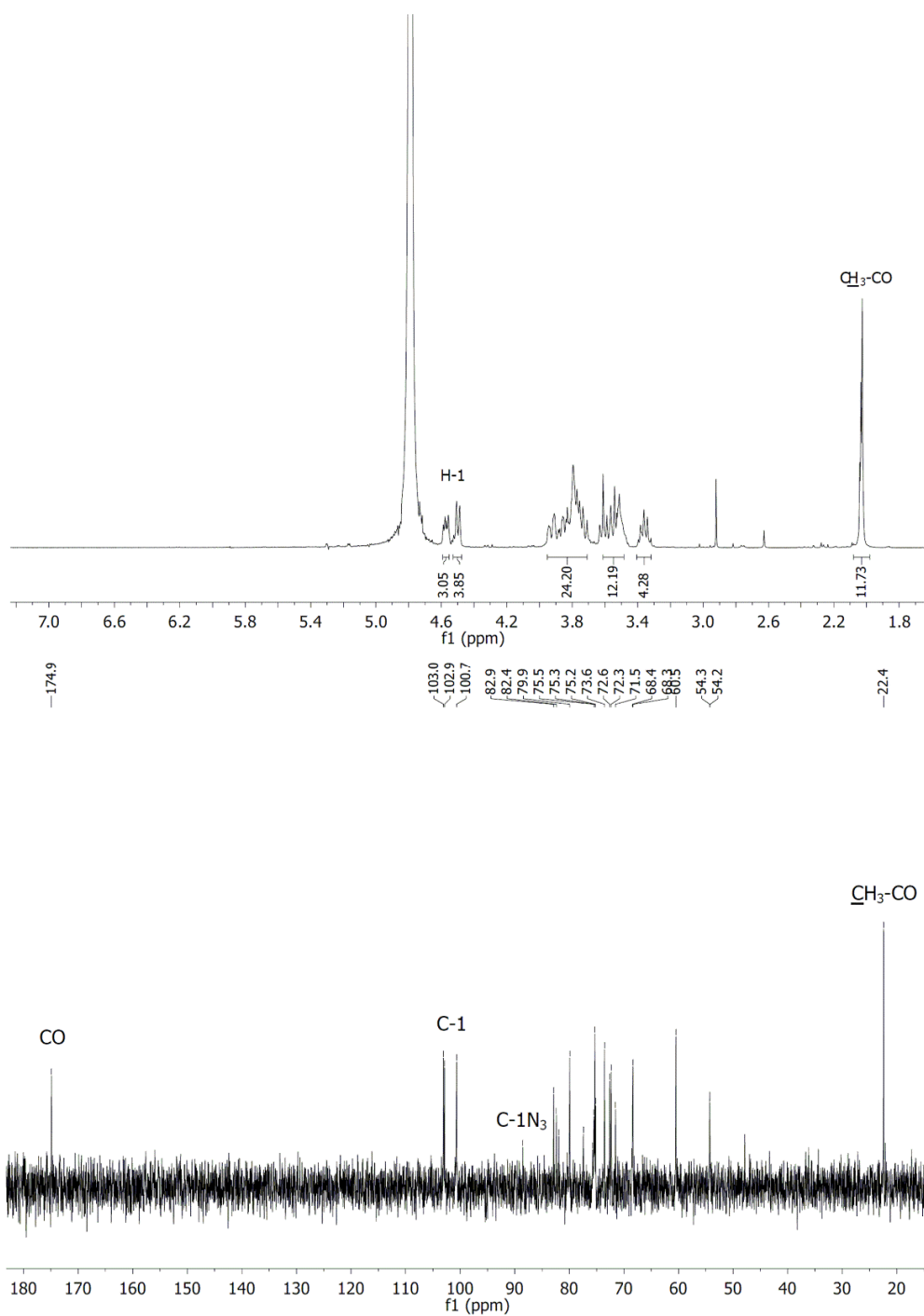


203 Sodium hyaluronate (HA) was incubated with bovine testes hyaluronidase (BTH), an  
204 enzyme known for degrading HA to oligosaccharides. As BTH does not accept  
205 tetrasaccharides as substrates (Mahoney, Aplin, Calabro, Hascall, & Day, 2001) extensive  
206 enzymatic hydrolysis lead to the DP4 as the main product. We managed the reaction  
207 conditions in order to obtain a mixture of oligosaccharides.

208 A preparative HPAEC-ELSD was used to purify the oligosaccharides, using a DEAE-cellulose  
209 column and a gradient of aqueous solution of ammonium formate from 1mM to 1M as  
210 eluent. The main compounds of the mixture were eluted at 23.7 (DP4, **1a**), 28.6 (DP6, **1b**)  
211 and 32.7 min (DP8, **1c**) (Figure S1). After lyophilization, they were obtained in 14%, 16%  
212 and 17% yield, respectively. The analytical data of these oligosaccharides were in  
213 accordance with previous reported data (Blundell, Reed, & Almond, 2006; Tawada et al.,  
214 2002) (Figures S3-S5 and Table S1).

### 215 *3.2. Synthesis of the phospholipo-oligohyaluronates*

216 In order to study the impact of the length of the sugar residue in the liposomes, the  
217 oligohyaluronans were modified to perform the synthesis of the amphiphilic compounds.  
218 As shown in Scheme 1, a direct azidation of anomeric position was performed with 2-  
219 chloro-1,3-dimethylimidazolinium (DMC), *N*-methylmorpholine and NaN<sub>3</sub> in water at 0 °C.  
220 Compounds **2a**, **2b** and **2c** were obtained in 68%, 65% and 63% yield, respectively. <sup>13</sup>C  
221 NMR spectra of compounds **2a**, **2b** and **2c** showed the diagnostic signal at 88.5 ppm  
222 corresponding to the C1-N<sub>3</sub> (Figure 1).



223

224 **Figure 1.**  $^1\text{H}$  NMR (400 MHz) (top) and  $^{13}\text{C}$  NMR (101 MHz) (bottom) spectra of compound

225 **2c** recorded in  $\text{D}_2\text{O}$  in a Bruker DRX 400.



239 linked to the surface of preformed liposomes by covalent conjugation between the  
240 carboxylic residues of HA and phospholipid amine groups (Yerushalmi, Arad, & Margalit,  
241 1994). This method offers the advantage to conjugate HA only on the external surface of  
242 the particle but makes difficult the control the density of attachment of HA on the  
243 liposomes. In the second method HA oligomers are previously conjugated to a lipid anchor  
244 permitting the introduction of the conjugate into the lipid mixture during liposomes  
245 preparation in a controlled amount (Arpicco et al., 2013; Eliaz & Szoka, 2001; Marengo et  
246 al., 2019; Ruhela, Kivima, & Szoka, 2014).

247 To the best of our knowledge our compounds are the first examples of conjugates  
248 composed of HA oligomers linked to PEG phospholipids. The presence of PEG should  
249 improve the targeting ability of the systems decreasing the steric hindrance of the  
250 liposomes in the ligand-receptor interaction.

251 The HA-DP4 (**4a**), HA-DP6 (**4b**) and HA-DP8 (**4c**) conjugates were added at a molar ratio of  
252 3 during hydration to a lipid film composed of DSPC/CHOL/mPEG2000-DSPE (75:20:2  
253 molar ratio). In this way, the phospholipidic chain was **completely** incorporated into the  
254 liposome membrane, while the HA was exposed toward the aqueous phase; for  
255 comparison plain liposomes were prepared without adding the conjugates. The  
256 physicochemical characteristics of the different formulations are summarized in Table 1.  
257 Liposomes displayed a dimensional range of about 160 nm and the polydispersity index  
258 was low for all the formulations (< 0.18). Liposomes showed a negative Zeta potential  
259 value that was lower for decorated liposomes compared to plain ones, due to the  
260 carboxylic negative residues of conjugates. In particular, the negative charge slightly  
261 increased as the conjugate MW increased confirming the presence of glycoconjugates on  
262 the surface of the liposomes.

### 263 **Table 1**

264 Characteristics of plain and decorated liposomes. Values are the means  $\pm$  SEM of three  
265 independent experiments each performed in triplicate.

Phospholipid composition	Mean particle size (nm)	Polydispersity index	Zeta potential (mV)
<b>PLAIN</b> DSPC/Chol/mPEG-DSPE 75:20:2	163 ± 1.3	0.115	-9.3 ± 0.8
<b>HA-DP4</b> DSPC/Chol/mPEG-DSPE/ <b>4a</b> 75:20:2:3	166 ± 1.5	0.175	-27.1 ± 1.1
<b>HA-DP6</b> DSPC/Chol/mPEG-DSPE/ <b>4b</b> 75:20:2:3	165 ± 1.8	0.166	-32.6 ± 1.9
<b>HA-DP8</b> DSPC/Chol/mPEG-DSPE/ <b>4c</b> 75:20:2:3	166 ± 1.6	0.149	-35.3 ± 2.1
<b>HA-4800</b> DSPC/Chol/mPEG-DSPE/HA-4800 75:20:2:3	176 ± 2.1	0.121	-19.3 ± 1.6
<b>HA-14800</b> DSPC/Chol/mPEG-DSPE/HA-1480075:20:2:3	195 ± 2.4	0.175	-20.7 ± 1.4

266

267 *3.4. Cellular uptake, viability and inflammatory profile*

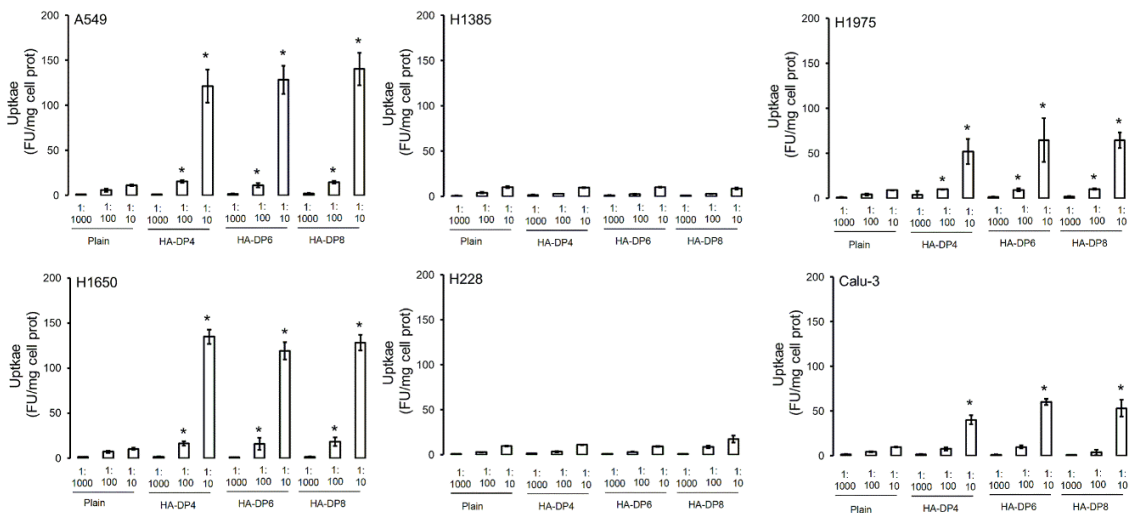
268 *3.4.1 Cellular uptake*

269 We preliminary screened different human non-small cell lung cancer cell lines for their  
 270 expression of CD44, the receptor of HA, in comparison with non-transformed epithelial  
 271 lung cells BEAS-2B. While CD44 was poorly expressed in BEAS-2B cells, in the cancer cell  
 272 lines analyzed we detected cells with high (A549, NCI-H1650), moderate (NCI-H1975, Calu-  
 273 3) and low CD44 expression (NCI-H1385, NCI-H228) (Figure S2).

274 With the aim of understanding the significance of oligomer length for receptor binding,  
 275 we next evaluated the cellular uptake of the liposomes, by using fluorescently labelled  
 276 particles and measuring the intracellular accumulation of the fluorophore. All cell lines  
 277 displayed a dose-dependent uptake of the liposome cargo. In line with the different  
 278 expression of CD44, the uptake of HA-DP4, HA-DP6 and HA-DP8-decorated liposomes was  
 279 significantly higher in A549 and NCI-H1650 cells, and – to a lesser extent – in NCI-H1975  
 280 and Calu-3 cell, compared to plain liposomes. No differences in the uptake between

281 decorated and plain liposomes were detected in poorly expressing NCI-H1385 and NCI-  
 282 H228 cells (Figure 2). This experimental set suggests that the entry of HA-conjugated  
 283 formulations is likely receptor-mediated. Our hypothesis was confirmed by competition  
 284 assays performed on CD44<sup>high</sup> A549 and NCI-H1650 cells, incubated at different time  
 285 points with liposomes in the presence of a saturating amount of anti-CD44 antibody or  
 286 HA. As expected, the uptake increased over the time; such increase was higher with HA-  
 287 decorated liposomes than with plain liposomes. However, the presence of anti-CD44  
 288 antibody or HA blunted the uptake of HA-decorated liposomes (Figure 3).

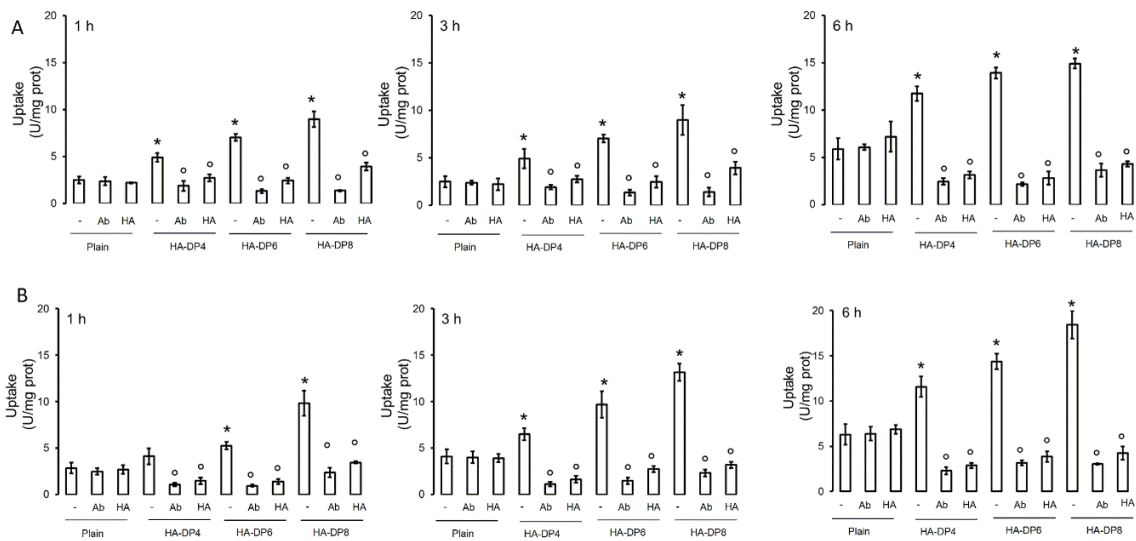
289



290

291 **Figure 2.** Cellular uptake of fluorescently labeled liposomes. A549, NCI-H1385, NCI-H1975,  
 292 NCI-H1650, NCI-H228, Calu-3 cells were incubated 24 h with fluorescently labelled plain  
 293 liposomes, HA-DP4-decorated, HA-DP6-decorated, HA-DP8-decorated liposomes, at a final  
 294 dilution in the culture medium of 1:10, 1:100, 1:1000. The intracellular content of  
 295 fluorescein, considered an index of liposome uptake, was measured  
 296 spectrofluorimetrically in triplicates. Data are means  $\pm$  SD (n = 4). \* p < 0.05: HA-  
 297 conjugated liposomes vs. corresponding plain liposomes.

298



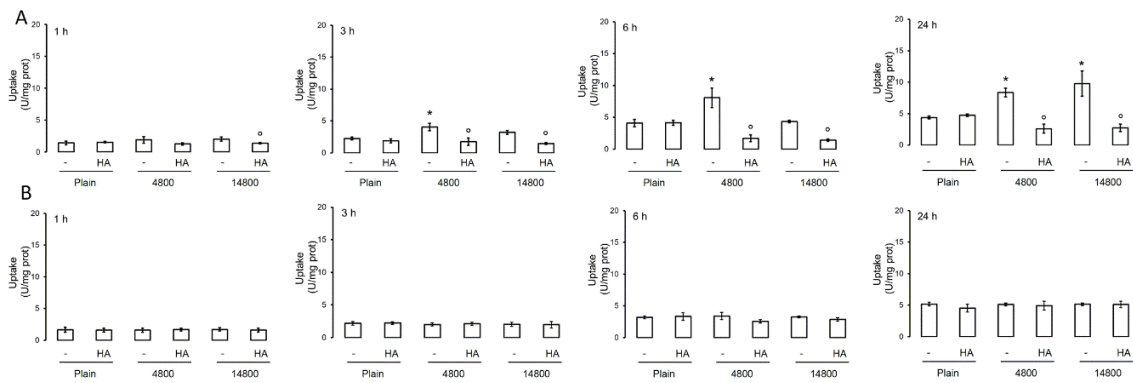
299

300 **Figure 3.** Competition assays in cellular uptake of fluorescently labeled liposomes. A549  
 301 (panel A) and NCI-H1650 (panel B) cells were incubated 1, 3 and 6 h with fluorescently  
 302 labelled plain liposomes, HA-DP4-decorated, HA-DP6-decorated, HA-DP8-decorated  
 303 liposomes, at a final dilution in the culture medium of 1:100, in the absence (-) or in the  
 304 presence of an anti-CD44 antibody (Ab, at a final dilution of 1:10) or HA (100  $\mu$ M). The  
 305 intracellular content of fluorescein, considered an index of liposome uptake, was  
 306 measured spectrofluorimetrically in triplicates. Data are means  $\pm$  SD (n = 4). \* p < 0.05:  
 307 conjugated liposomes vs. corresponding plain liposomes; ° p < 0.001: Ab-HA-treated  
 308 samples vs untreated (-) samples.

309 Interestingly, the amount of liposomes uptake at each time point followed this rank order:  
 310 HA-DP8>HA-DP6>HA-DP4 liposomes at 1, 3 and 6 h (Figure 3), suggesting that the HA-DP8  
 311 formulations were optimal in inducing a fast receptor binding and triggering a receptor-  
 312 mediated endocytosis.

313 To better compare the kinetics of entry of the liposomes with the structure of the  
 314 conjugates used for their decoration, we analyzed the time-dependent uptake of  
 315 liposomes prepared using conjugates previously synthesized in our laboratory (Arpicco et  
 316 al., 2013) obtained by linking HA with two different molecular weight (4800 and 14800 Da)

317 to an aminated phospholipid by reductive amination. For this purpose, we used the highly  
 318 CD44-expressing A549 cells and the poorly CD44-expressing NCI-H228 cells. While in the  
 319 latter cell lines, there was always a lower uptake that did not change upon the time nor in  
 320 presence of an excess of HA, in A549 cells we observed that HA-4800 conjugates were  
 321 more taken up than HA-14800 conjugates at early time-points (1, 3 and 6 h). The  
 322 difference was not maintained at 24 h. After 3, 6 and 24 h, the uptake was drastically  
 323 reduced by HA in A549 cells, confirming that the intracellular delivery was CD44-  
 324 dependent (Figure 4).



325

326 **Figure 4.** Competition assays in cellular uptake of fluorescently labeled liposomes with  
 327 high and low molecular weight HA. A549 (panel A) and NCI-H228 (panel B) cells were  
 328 incubated 1, 3, 6 and 24 h with fluorescently labelled plain liposomes, HA 4800 and HA  
 329 14800 liposomes, at a final dilution in the culture medium of 1:100, in the absence (-) or in  
 330 the presence of HA (100  $\mu$ M). The intracellular content of fluorescein, considered an index  
 331 of liposome uptake, was measured spectrofluorimetrically in triplicates. Data are means  $\pm$   
 332 SD (n = 4). \* p < 0.05: conjugated liposomes vs. corresponding plain liposomes; ° p < 0.05:  
 333 HA-treated samples vs untreated (-) samples.

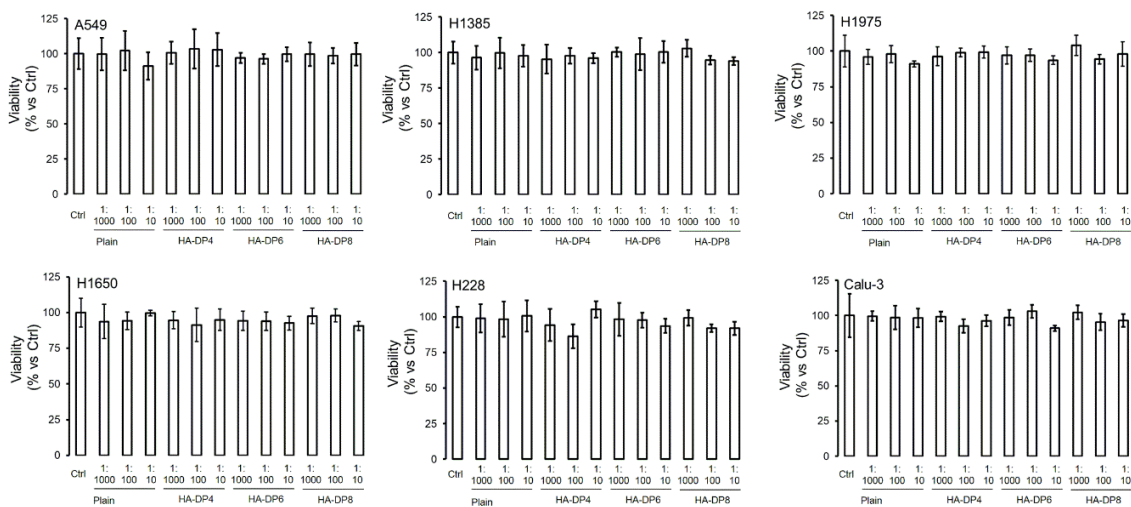
334 This trend likely suggests that HA-DP4, 6 and 8 conjugates are capable of a faster  
 335 interaction with CD44, followed by phagocytosis, while the entry of the other HA-  
 336 conjugated liposomes requires more time. The sterical hindrance that makes the HA/CD44  
 337 interaction more complex and/or the need of CD44 clusterization upon the binding of



338 higher molecular weight HA conjugates may explain this difference. The presence of a PEG  
 339 chain between the phospholipid and the HA oligomer in our conjugates should also  
 340 improve the uptake. Moreover, at the same time point and in the same cell line, *i.e.* in the  
 341 presence of the same amount of CD44, the uptake of both 4,800-HA and 14,800-HA  
 342 conjugates was lower than the uptake of HA-DP4, the less effective conjugate in cellular  
 343 delivery (Figure 2, 3 and 4).

### 344 3.4.2. Cell viability and inflammatory profile

345 We finally analyzed the biocompatibility of our formulations. After 72 h incubation, either  
 346 unconjugated or HA-conjugated liposomes did not significantly reduce cell viability, in  
 347 both CD44<sup>low</sup> and CD44<sup>high</sup> cells (Figure 5). In parallel, none of the formulations changed  
 348 the expression of pro-inflammatory cytokines more than two-fold compared to untreated  
 349 cells (Figure 6). These two results suggest that in our experimental conditions the  
 350 liposomes are not cytotoxic and do not increase the release of potentially pro-  
 351 inflammatory mediators. DP4-20 have pro-inflammatory properties in biological systems  
 352 (Gao et al., 2008) and this side-effect may strongly limit the potential therapeutic  
 353 application of HA-conjugates. Our results suggest the safety – in terms of lack of  
 354 cytotoxicity and inflammatory effects – of HA-DP4, HA-DP6 and HA-DP8-liposomes,  
 355 opening the perspective of their employment in nanomedicine.



356

357 **Figure 5.** Viability of cells treated with liposomes. A549, NCI-H1385, NCI-H1975, NCI-  
 358 H1650, NCI-H228, Calu-3 cells were incubated 72 h with fresh medium (Ctrl) or with  
 359 medium containing plain liposomes, HA-DP4-decorated, HA-DP6-decorated, HA-DP8-  
 360 decorated liposomes, at a final dilution in the culture medium of 1:10, 1:100, 1:1000. Cell  
 361 viability was measured by a chemiluminescence-based assay in quadruplicates. Data are  
 362 means  $\pm$  SD (n =4).

Cell	Plain	HA-DP4	HA-DP6	HA-DP8	Cell	Plain	HA-DP4	HA-DP6	HA-DP8	Cell	Plain	HA-DP4	HA-DP6	HA-DP8	Cell	Plain	HA-DP4	HA-DP6	HA-DP8										
A549	1.2	1.4	1.2	1.5	H1385	1.1	1.2	1.2	1.1	H1975	0.9	1	1.2	1.3	H1650	0.8	1	1.1	0.9	H228	1.1	1	1	0.9	Calu-3	1.2	1.3	1.2	1.1
Eotaxin	1.4	1.4	1.4	1.3	Eotaxin-2	0.9	0.9	1	1.2	Eotaxin-2	0.9	0.9	1	1.2	Eotaxin	0.8	1	1.1	0.9	Eotaxin	1.1	1	1	0.9	Eotaxin-2	1.2	1.1	1.3	1.2
GM-CSF	0.7	0.7	0.8	0.9	GM-CSF	1.2	1.1	1.4	1.2	GM-CSF	1.1	1.2	1.3	1	GM-CSF	0.9	0.8	0.9	0.8	GM-CSF	1	0.9	0.9	1.1	GM-CSF	0.8	0.9	1	1.1
ICAM-1	0.8	1	0.8	0.9	ICAM-1	1.4	1.3	1.2	1.1	ICAM-1	1.3	1.2	1.4	1.2	ICAM-1	0.9	0.7	0.7	0.8	ICAM-1	1.2	1.1	1	1	ICAM-1	1	1.1	1.2	1
IP3gamma	1.1	1.3	1.4	1.3	IP3gamma	1	1	1.2	1.3	IP3gamma	1.2	0.8	0.9	1	IP3gamma	1.2	1.1	1	0.9	IP3gamma	1	1.2	1.3	1.2	IP3gamma	1.1	1.2	1.3	1.2
I309	1.8	1.6	1.6	1.5	I309	1.4	1.3	1.3	1.2	I309	1.3	1.5	1.3	1	I309	1	1.1	1.4	1.2	I309	1.3	1.3	0.9	0.9	I309	1.1	1.2	1	1
IL-1alpha	1.3	1.4	1.4	1.3	IL-1alpha	1.4	1.4	1.3	1.1	IL-1alpha	1	1	1.1	1.2	IL-1alpha	1.3	1.4	1.3	1.3	IL-1alpha	1.1	1.2	1	1.2	IL-1alpha	1.2	1.3	1.2	1.1
IL-1beta	1.4	1.6	1.5	1.5	IL-1beta	1.1	1.2	1.1	1.3	IL-1beta	1.2	1.3	1.4	1	IL-1beta	1.4	1.2	1.5	1.2	IL-1beta	1.2	1.1	1.2	1.1	IL-1beta	1.2	1.1	1	1.1
IL-2	1.7	1.8	1.7	1.7	IL-2	1.3	1.1	1.1	1	IL-2	0.6	1	1.1	1.2	IL-2	1.2	1.3	1.2	1.1	IL-2	1.1	0.9	0.9	1	IL-2	1.1	1.2	1	0.9
IL-3	1.6	1.6	1.4	1.5	IL-3	1.4	1.3	1.4	1.3	IL-3	1	1.2	0.9	0.9	IL-3	1.1	1.2	1.3	1.3	IL-3	1	1.2	1.3	1.2	IL-3	1	1.2	0.8	1.1
IL-4	1.2	0.9	1.3	1.3	IL-4	1.2	1	0.9	0.8	IL-4	1.3	1.1	1.2	1.1	IL-4	1.2	1.3	1.1	1	IL-4	1.1	1	1.1	1.1	IL-4	1.3	1	1.1	0.9
IL-5	1	0.9	1	0.9	IL-5	1.4	1.2	1.1	1	IL-5	1.2	1.1	1.3	1.2	IL-5	1.1	0.9	1.2	1.1	IL-5	1.3	1.2	1.1	1.2	IL-5	1.2	1.1	1	1
IL-6aR	0.4	0.5	0.7	0.7	IL-6aR	1	1.3	0.8	0.9	IL-6aR	1.3	1.2	1.2	1.1	IL-6aR	1	0.8	0.8	0.9	IL-6aR	1.1	1	1.2	1.2	IL-6aR	1.3	1	1.2	1.2
IL-7	0.9	0.9	0.7	0.5	IL-7	1.1	1.2	1.3	1	IL-7	1.3	1.2	1.1	1.2	IL-7	0.9	0.9	0.8	1	IL-7	1.3	1.1	1	1	IL-7	1.2	1.3	1	1.2
IL-8	0.4	0.5	0.4	0.4	IL-8	1	1.2	1	1.2	IL-8	1.1	1.2	1.2	1	IL-8	1	1.2	1	0.8	IL-8	1	1	1.2	0.9	IL-8	1.1	1.3	1.4	1.3
IL-9	0.7	0.8	0.9	0.7	IL-9	1.3	1.1	1.2	1.3	IL-9	0.9	0.9	1	1.2	IL-9	0.9	1.1	1	0.9	IL-9	1.1	0.9	1	1.2	IL-9	1.2	1.2	1.2	1
IL-10	0.9	0.8	0.9	1.3	IL-10	1.1	1	1.3	1.1	IL-10	1.2	1	1.2	1.2	IL-10	0.9	1.1	0.8	0.9	IL-10	1.3	1.2	1	1.1	IL-10	1.1	1.1	1.2	1.3
IL-11	1.2	1.5	1.4	1.5	IL-11	1.2	1.1	1	0.8	IL-11	1.1	1.3	1	1.2	IL-11	1.2	1	0.9	0.7	IL-11	1.2	1.1	1.3	1.1	IL-11	1.2	1.1	1.2	1.3
IL-12p40	1.3	1.6	1.2	1.3	IL-12p40	1.2	0.9	0.9	0.8	IL-12p40	1.2	1.3	1	1.1	IL-12p40	1.2	1	1.2	1.1	IL-12p40	1.2	1.1	1.1	1	IL-12p40	1.1	1.3	1.1	1.2
IL-13	1.3	1.8	1.3	1.5	IL-13	1.1	1	1	1.3	IL-13	0.9	0.8	1.1	0.9	IL-13	1.1	1.3	1.4	1.5	IL-13	1.1	0.9	0.8	0.9	IL-13	1.2	1.1	0.9	0.9
IL-15	1.8	1.7	1.7	1.3	IL-15	1.2	1	1.1	1.3	IL-15	1	1.2	1	0.9	IL-15	1.2	1.3	1.4	1	IL-15	1.2	1.1	1	1.1	IL-15	1	1.2	1.1	1.2
IL-16	1.9	1.6	1.6	1.5	IL-16	1	1.3	1.2	1.1	IL-16	0.8	0.9	1.1	1.2	IL-16	1.1	1.2	1.3	1.2	IL-16	1.2	1.1	1.2	1	IL-16	1.2	1	1	1.3
IL-17	1.2	1.4	1.2	1.3	IL-17	1.2	1.3	0.9	1	IL-17	1.1	1.2	1	1.3	IL-17	1.2	1.2	1.3	1.4	IL-17	1	1.1	1.2	1.1	IL-17	1.1	1.4	1.3	1.2
IP-10	1	0.9	0.9	1.5	IP-10	1.2	1	1.3	1.1	IP-10	1.2	1.1	1.3	1.4	IP-10	1	1	1.1	1.3	IP-10	1	1.1	1.2	1	IP-10	1.2	1.3	1.2	1
MCP-1	1.1	1.7	1.3	1.4	MCP-1	1.2	1	1.2	1.1	MCP-1	0.9	1	1.1	1.2	MCP-1	0.9	1	1	0.9	MCP-1	1.1	1.2	0.8	0.9	MCP-1	0.8	1.1	0.9	1.1
MCP-2	0.7	1.6	1.4	1.5	MCP-2	1.3	1.4	1.2	1	MCP-2	1	1.1	1.3	1	MCP-2	0.9	1	1.1	0.8	MCP-2	1.2	1.1	1.1	1	MCP-2	1.2	1.1	1	1.2
MCSF	1.3	1.4	1.3	1.2	MCSF	1.2	1.3	1.3	1.1	MCSF	1.2	1.1	1.2	1.1	MCSF	1.1	1.2	1.3	MCSF	0.9	1.1	1.2	1.2	MCSF	1	1.2	1.1	1.1	
MIG	1.5	1.8	1.8	1.5	MIG	1.1	1.2	1	0.9	MIG	1.3	1.1	1.1	0.9	MIG	1.3	1.4	1.2	1.1	MIG	1.1	0.9	1.2	1.1	MIG	1.2	1.1	1	1.1
MP-1alpha	1.2	1.3	1.3	1.4	MP-1alpha	0.9	1.1	1.2	1	MP-1alpha	1.1	1	0.9	1.2	MP-1alpha	1.1	1.2	1.4	1.2	MP-1alpha	1.1	1.1	1.2	1	MP-1alpha	1.2	1.1	1.1	1.2
MP-1beta	1.5	1.6	1.4	1.1	MP-1beta	1	1.1	1.3	1.2	MP-1beta	1.1	1.2	1	1.3	MP-1beta	1.1	1.2	1.1	1.2	MP-1beta	1.1	1	1.2	0.9	MP-1beta	1.2	1.3	1	1.1
MP-1delta	1.3	0.7	1.2	1.3	MP-1delta	1	1	0.8	0.9	MP-1delta	1	0.9	0.9	0.8	MP-1delta	1.2	1.1	1	1.3	MP-1delta	1.1	1.2	1.3	1.1	MP-1delta	1.1	1.2	1.3	1.2
RANTES	1.3	0.8	0.8	0.9	RANTES	1.2	1.1	1.2	1.1	RANTES	1.2	1.1	1	1.1	RANTES	1.2	1.1	1.2	1.1	RANTES	1.1	1	1.2	1	RANTES	1.1	1.2	1.3	1.1
TGF-beta1	1.8	1.8	1.7	1.3	TGF-beta1	1.1	1.2	1.1	1.2	TGF-beta1	1.2	1.3	1	1.1	TGF-beta1	0.9	0.8	0.8	1	TGF-beta1	1.1	0.9	0.9	0.9	TGF-beta1	1.1	1.2	1.3	1.1
TNF-alpha	0.9	1.6	1.4	1.5	TNF-alpha	1	0.8	0.9	1	TNF-alpha	1.2	0.9	0.8	0.7	TNF-alpha	0.9	0.7	0.8	0.8	TNF-alpha	1.1	1	0.9	0.8	TNF-alpha	1.1	1.3	1.2	1.1
TNF-beta	0.7	1.4	1.2	1.3	TNF-beta	1.1	0.9	0.9	1	TNF-beta	0.9	0.8	1	1.1	TNF-beta	0.9	1	0.9	0.8	TNF-beta	1.2	0.9	0.9	0.8	TNF-beta	1.2	1.2	1.1	1.2
sTNF-RI	1	1.4	1.8	1.5	sTNF-RI	1.2	1.3	1.3	1.2	sTNF-RI	1.2	1.3	1.2	1.2	sTNF-RI	1.2	1.1	1.2	1.4	sTNF-RI	1.1	1.2	1	0.9	sTNF-RI	1.1	1.3	1.2	1.1
sTNF-RII	1.1	1.6	1.3	1.1	sTNF-RII	1.2	1.4	1.2	1.3	sTNF-RII	1.1	1.2	1	0.9	sTNF-RII	1.2	1.2	1.3	1	sTNF-RII	1.1	1.2	1.1	1.2	sTNF-RII	1.2	1.1	1.2	1.2
PDGF-BB	1.6	1.8	1.3	1.1	PDGF-BB	1.1	1.2	1.2	1.4	PDGF-BB	0.9	1.2	1	1.2	PDGF-BB	1.3	1.1	1.3	1.2	PDGF-BB	1	1.1	1.1	1.2	PDGF-BB	1	0.9	0.9	1.1
TMP-2	1.3	1.3	1.4	1.2	TMP-2	1	0.9	0.8	1.2	TMP-2	0.8	0.9	1.2	1.1	TMP-2	1.1	1.2	1.1	1.2	TMP-2	1	1.3	1.2	1	TMP-2	1.2	1.1	0.9	1.1

364 **Figure 6.** Cytokine production from cells treated with liposomes. A549, NCI-H1385, NCI-  
 365 H1975, NCI-H1650, NCI-H228, Calu-3 were incubated 72 h with fresh medium (Ctrl) or  
 366 with medium containing plain liposomes, HA-DP4-decorated, HA-DP6-decorated, HA-DP8-  
 367 decorated liposomes, at a final dilution of 1:10. 1 ml of the culture medium was subjected  
 368 to the detection of cytokines by antibody arrays. The dot blot density of untreated cells  
 369 was considered 1; results of the treatment conditions were expressed as fold change  
 370 (density of dot blot for each experimental condition/density of dot blot in untreated cells  
 371 for the same cytokine), using a heatmap.

372 Indeed, exploiting the abundance of CD44 in non-small cell lung cancers (Chen, Zhao,  
 373 Karnad, & Freeman, 2018; Penno et al., 1994), HA decorated liposomes can be used for  
 374 the active targeting of anti-cancer drugs. Resistance to conventional chemotherapeutic  
 375 agents (Chang, 2011) or targeted-therapies used in specific patients subsets with  
 376 oncogenic mutations (Leonetti et al., 2018) is still a challenge in the therapeutic approach

377 of non-small cell lung cancers. The active targeting of tumors using anti-cancer drugs  
378 encapsulated in liposomes is more effective than the administration of free drugs against  
379 drug resistant tumors (Nag & Delehanty, 2019). This approach can improve in particular  
380 the efficacy and pharmacokinetic profile of first-line drug in non-small cell lung cancers  
381 such as cisplatin (Zhong et al., 2020). After evaluating the technical feasibility and binding  
382 of our conjugates, we are next planning to load suitable anti-cancer drugs, deeply  
383 characterize the formulations and evaluate their safety and anti-tumor efficacy against  
384 CD44-expressing non-small cell lung cancers.

#### 385 **4. Conclusions**

386 Novel conjugates between HA oligomers of different DP (4, 6 and 8) and PEGylated  
387 phospholipid were prepared via click chemistry of 1-azido oligohyaluronates and  
388 azadibenzocyclooctyne phospholipid. These conjugates were introduced during the  
389 preparation of liposomes that were characterized in terms of size and zeta potential.

390 In order to evaluate their targeting *in vitro* studies on lung cancer cell lines with different  
391 expression of CD44 were done, to assess the ability of cellular delivery and the lack of  
392 toxicity or pro-inflammatory effects. This study is a proof of concept of the feasibility and  
393 biocompatibility of HA-conjugates, and opens the way to their future development as  
394 active-targeting agents carrying anti-tumor drugs.

#### 395 **Supplementary material**

396 Purification of oligohyaluronates, surface expression of CD44 in lung cells and NMR  
397 spectra and HRMS of compounds **1a**, **1b** and **1c**.

#### 398 **Acknowledgments**

399 This work was supported by the Centre National de la Recherche Scientifique (CNRS),  
400 l'Université de Picardie Jules Verne, the Agence Nationale de la Recherche (ANR-18-SUS2-

401 0001, France) and by the Italian Ministry for University and Research (MIUR)—University  
402 of Torino, “Fondi Ricerca Locale (ex-60%)”

### 403 **References**

- 404 Arpicco, S., Lerda, C., Dalla Pozza, E., Costanzo, C., Tsapis, N., Stella, B., ... Palmieri, M.  
405 (2013). Hyaluronic acid-coated liposomes for active targeting of gemcitabine.  
406 *European Journal of Pharmaceutics and Biopharmaceutics*, *85*(3 Part A), 373–380.  
407 <https://doi.org/10.1016/j.ejpb.2013.06.003>
- 408 Blundell, C. D., Reed, M. A. C., & Almond, A. (2006). Complete assignment of hyaluronan  
409 oligosaccharides up to hexasaccharides. *Carbohydrate Research*, *341*(17), 2803–2815.  
410 <https://doi.org/10.1016/j.carres.2006.09.023>
- 411 Chang, A. (2011). Lung Cancer Chemotherapy, chemoresistance and the changing  
412 treatment landscape for NSCLC. *Lung Cancer*, *71*(1), 3–10.  
413 <https://doi.org/10.1016/j.lungcan.2010.08.022>
- 414 Chen, C., Zhao, S., Karnad, A., & Freeman, J. W. (2018). The biology and role of CD44 in  
415 cancer progression : therapeutic implications. *Journal of Hematology & Oncology*,  
416 *11*(64), 1–23. <https://doi.org/10.1186/s13045-018-0605-5>
- 417 Dalla Pozza, E., Lerda, C., Costanzo, C., Donadelli, M., Dando, I., Zoratti, E., ... Palmieri, M.  
418 (2013). Targeting gemcitabine containing liposomes to CD44 expressing pancreatic  
419 adenocarcinoma cells causes an increase in the antitumoral activity. *BBA -*  
420 *Biomembranes*, *1828*(5), 1396–1404. <https://doi.org/10.1016/j.bbamem.2013.01.020>
- 421 Dosio, F., Arpicco, S., Stella, B., & Fattal, E. (2016). Hyaluronic acid for anticancer drug and  
422 nucleic acid delivery. *Advanced Drug Delivery Reviews*, *97*, 204–236.  
423 <https://doi.org/10.1016/j.addr.2015.11.011>
- 424 Eliaz, R. E., & Szoka, F. C. (2001). Liposome-encapsulated Doxorubicin Targeted to CD44 : A  
425 Strategy to Kill CD44-overexpressing Tumor Cells. *Cancer Research*, *61*, 2592–2601.
- 426 Fuster, M. M., & Esko, J. D. (2005). THE SWEET AND SOUR OF CANCER : GLYCANS AS  
427 NOVEL THERAPEUTIC TARGETS. *Nature Reviews Cancer*, *5*, 526–542.

428 <https://doi.org/10.1038/nrc1649>

429 Gao, F., Yang, C. X., Mo, W., Liu, Y. W., & He, Y. Q. (2008). Hyaluronan oligosaccharides are  
430 potential stimulators to angiogenesis via RHAMM mediated signal pathway in wound  
431 healing. *Clinical and Investigative Medicine*, 31(3), 106–116.  
432 <https://doi.org/10.25011/cim.v31i3.3467>

433 Gazzano, E., Buondonno, I., Marengo, A., Rolando, B., Chegaev, K., Kopecka, J., ... Riganti,  
434 C. (2019). Hyaluronated liposomes containing H2S-releasing doxorubicin are effective  
435 against P-glycoprotein-positive / doxorubicin-resistant osteosarcoma cells and  
436 xenografts. *Cancer Letters*, 456, 29–39. <https://doi.org/10.1016/j.canlet.2019.04.029>

437 Köhling, S., Blaszkiewicz, J., Ruiz-Gómez, G., Fernández-Bachiller, M. I., Lemmnitzer, K.,  
438 Panitz, N., ... Rademann, J. (2019). Syntheses of defined sulfated oligohyaluronans  
439 reveal structural effects, diversity and thermodynamics of GAG-protein binding.  
440 *Chemical Science*, 10(3), 866–878. <https://doi.org/10.1039/c8sc03649g>

441 Köhling, S., Künze, G., Lemmnitzer, K., Bermudez, M., Wolber, G., Schiller, J., ... Rademann,  
442 J. (2016). Chemoenzymatic Synthesis of Nonasulfated Tetrahyaluronan with a  
443 Paramagnetic Tag for Studying Its Complex with Interleukin-10. *Chemistry - A  
444 European Journal*, 22(16), 5563–5574. <https://doi.org/10.1002/chem.201504459>

445 Leonetti, A., Assaraf, Y. G., Veltsista, D., El Hassouni, B., Tiseo, M., & Giovannetti, E. (2018).  
446 MicroRNAs as a drug resistance mechanism to targeted therapies in EGFR- mutated  
447 NSCLC: current implications and future directions. *Drug Resistance Updates*, 42, 1–  
448 11. <https://doi.org/10.1016/j.drug.2018.11.002>

449 Mahoney, D. J., Aplin, R. T., Calabro, A., Hascall, V. C., & Day, A. J. (2001). Novel methods  
450 for the preparation and characterization of hyaluronan oligosaccharides of defined  
451 length. *Glycobiology*, 11(12), 1025–1033. <https://doi.org/10.1093/glycob/11.12.1025>

452 Marengo, A., Forciniti, S., Dando, I., Dalla, E., Stella, B., Tsapis, N., ... Palmieri, M. (2019).  
453 Pancreatic cancer stem cell proliferation is strongly inhibited by  
454 diethyldithiocarbamate- copper complex loaded into hyaluronic acid decorated  
455 liposomes Alessandro. *BBA - General Subjects*, 1863(1), 61–72.

456 <https://doi.org/10.1016/j.bbagen.2018.09.018>

457 Nag, O. K., & Delehanty, J. B. (2019). Active Cellular and Subcellular Targeting of  
458 Nanoparticles for Drug Delivery. *Pharmaceutics*, *11*(10), 543–570.  
459 <https://doi.org/10.3390/pharmaceutics11100543>

460 Penno, M. B., August, J. T., Baylin, S. B., Mabry, M., Linnoila, R. I., Lee, V. S., ... Rosada, C.  
461 (1994). Expression of CD44 in Human Lung Tumors. *Cancer Research*, *54*, 1381–1388.

462 Ruhela, D., Kivima, S., & Szoka, F. C. (2014). Chemoenzymatic Synthesis of Oligohyaluronan  
463 – Lipid Conjugates. *Bioconjugate Chemistry*, *25*, 718–723.  
464 <https://doi.org/10.1021/bc4005975>

465 Tawada, A., Masa, T., Oonuki, Y., Watanabe, A., Matsuzaki, Y., & Asari, A. (2002). Large-  
466 scale preparation, purification, and characterization of hyaluronan oligosaccharides  
467 from 4-mers to 52-mers. *Glycobiology*, *12*(7), 421–426.  
468 <https://doi.org/10.1093/glycob/cwf048>

469 Toole, B. P. (2004). HYALURONAN : FROM EXTRACELLULAR GLUE TO PERICELLULAR CUE.  
470 *Nature Reviews Cancer*, *4*, 528–539. <https://doi.org/10.1038/nrc1391>

471 Yang, C., Cao, M., Liu, H., He, Y., Xu, J., Du, Y., ... Gao, F. (2012). The High and Low  
472 Molecular Weight Forms of Hyaluronan Have Distinct Effects on CD44 Clustering \* □.  
473 *The Journal of Biological Chemistry*, *287*(51), 43094–43107.  
474 <https://doi.org/10.1074/jbc.M112.349209>

475 Yerushalmi, N., Arad, A., & Margalit, R. (1994). Molecular and Cellular Studies of  
476 Hyaluronic Acid-Modified Liposomes as Bioadhesive Carriers for Topical Drug Delivery  
477 in Wound Healing. *Archives of Biochemistry and Biophysics*, *313*(2), 267–273.  
478 <https://doi.org/10.1006/abbi.1994.1387>

479 Zhong, Y., Jia, C., Zhang, X., Liao, X., Yang, B., Cong, Y., ... Gao, C. (2020). European Journal  
480 of Medicinal Chemistry Targeting drug delivery system for platinum ( IV ) -Based  
481 antitumor complexes. *European Journal of Medicinal Chemistry*, *194*, 112229.  
482 <https://doi.org/10.1016/j.ejmech.2020.112229>